

Cryogenic Dark Matter Search: limits and projections

Priscilla Cushman for the CDMS Collaboration

School of Physics and Astronomy
University of Minnesota
116 Church St SE, Minneapolis, MN 55455 USA

E-mail: prisca@physics.umn.edu

Abstract. The results from the second run of the Cryogenic Dark Matter Search experiment in the Soudan Underground Laboratory yields new exclusion limits on the coherent WIMP-nucleon scalar cross-sections for WIMP masses above 15 GeV/c². Two towers, each consisting of six detectors, were operated in the mine for 74.5 live days, doubling the previous Ge exposure to 34 kg-d after cuts for recoil energies of 10-100 keV. When combined with the data from the first run at Soudan, the new upper limit is $1.6 \times 10^{-43} \text{ cm}^2$ for a 60 GeV WIMP using the standard dark-matter halo and nuclear physics WIMP model. This is a factor of 2.5 lower than our previous limit and a factor of 10 lower than any other experiment. Limits from the Si data (12 kg-d) are less stringent, but extend the excluded region for low mass WIMPs. CDMS also has sensitivity to spin-dependent limits.

1. Introduction

A central problem in cosmology and astrophysics today is the identity of the non-luminous matter in the Universe. A Concordance Model of cosmology has emerged over the past decade from studies of the microwave background, supernova and weak lensing, wherein the mass-energy density of the Universe is composed of 73% dark energy and only 27% matter, and where the matter in question is only 4% baryonic [1]. Non-baryonic or “dark” matter is indirectly observed via its effect on stellar motion in galaxies and clusters of galaxies. A direct detection would confirm its existence (ruling out arguments based solely on the modification of gravity), as well as define its properties.

Excellent candidates for dark matter are weakly-interacting relic particles from the Big Bang, the so-called WIMPs [2]. If supersymmetry is the correct extension of the Standard Model, one could interpret the nonbaryonic dark matter as its lightest stable neutral particle [3]. Supersymmetric models yield a wide range of neutralino mass and cross section predictions, much of which is accessible through direct detection experiments such as the Cryogenic Dark Matter Search (CDMS).

CDMS uses silicon and germanium detectors operated at $T < 50 \text{ mK}$ to detect energy deposited in the crystal by WIMPs which elastically scatter in the detector [4] as the earth moves through the dark matter halo. Moving at roughly 230 km/s relative to the detectors, WIMPs will impart a few keV to tens of keV kinetic energy to recoiling nuclei in the crystal. The CDMS detectors provide a wealth of information by which the resulting nuclear recoil can be distinguished from background events.

2. CDMS Detector and Readout

Each detector is 1 cm thick and 7.6 cm in diameter, and made of either high-purity germanium (250 g) or silicon (100 g). A schematic in figure 1 shows the 4 quadrants of phonon readout on the top surface. Each quadrant consists of 1,036 quasiparticle-assisted transition edge sensors operated in parallel. Each sensor consists of a 1 micron wide strip of tungsten connected to eight superconducting

aluminum collection fins. Its current is monitored by SQUIDs and maintained within the superconducting transition region by electrothermal feedback.

An applied electric field of a few volts/cm drifts the electron-hole pairs to the faces of the crystal. The ionization signal is then collected on the opposite face of the crystal by a disk-shaped inner electrode (Q-inner) of diameter 69 mm. An outer guard ring (Q-outer) separated by a 1 mm gap from the inner is used to reject events occurring near the edge of the crystal where the electric field is non-uniform and the detector not shielded by other detectors in the tower. Both phonon and charge signals are recorded with an effective 1.25 MHz sampling rate using waveform digitizers, resulting in the 6 traces shown to the right in figure 2. The sum of all 4 phonon channels is used to trigger data readout.

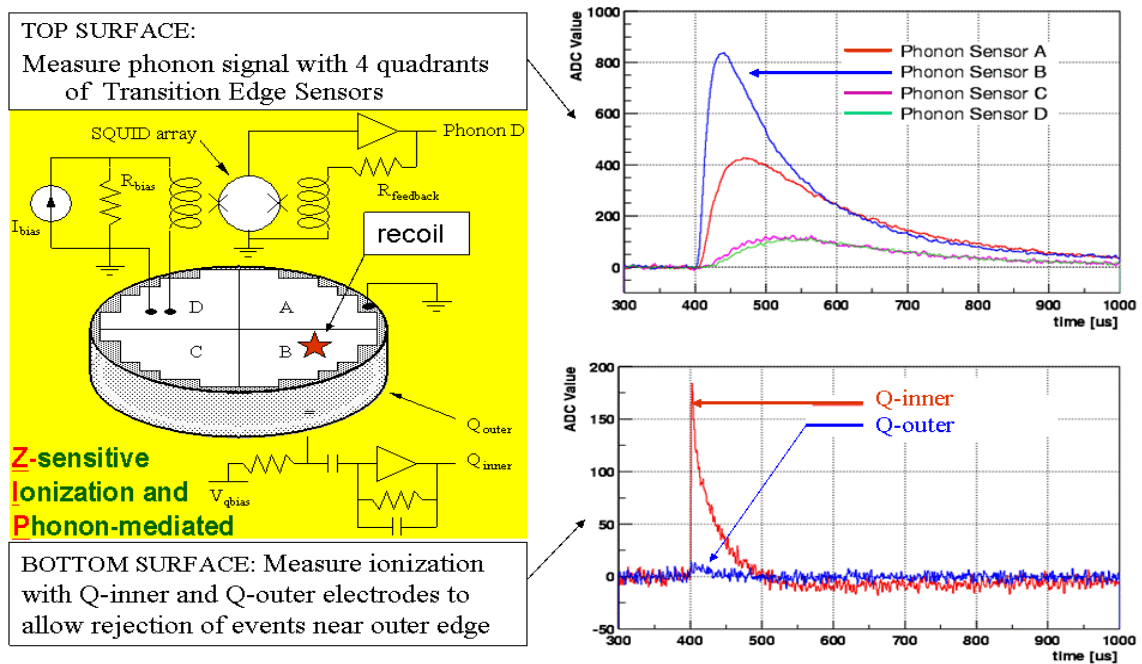


Figure 1. Left: Schematic of the CDMS detector showing the phonon readout on top and the ionization readout at the bottom. Right: Signals from a recoil event (star) in quadrant B.

Position information is available via the relative energy partition among the 4 phonon quadrants – note how the traces in figure 1 clearly show that the recoil happened in quadrant B, closer to quadrant A than to C or D. Another measure of position is found by comparing the relative phonon delay times of the peak sensor and its two neighbors. This information aids in diagnosis of detector problems, helps us gauge the success of the neutralization process (light injection clears the crystal of space-trapped charge), and determine position-dependent corrections to peak risetime and delay parameters which are used to distinguish between bulk and surface events.

The ratio of ionization to phonon recoil energy is called the “yield”, with electron recoils giving a yield normalized on average to one and nuclear recoils giving yields around 0.3. The top and bottom bands in figure 2 illustrate this distinction for calibration data taken with radioactive sources: ^{133}Ba for gammas (red dots) and ^{252}Cf for neutrons (blue circles). This is our primary means of eliminating gamma and beta background. The calibration data is used to determine the electron-recoil and nuclear-recoil yield by fitting the distributions to Gaussians in different recoil energy slices. Events within 2σ of the average lie within the band. Any WIMP should show up inside the nuclear-recoil band. In analyzing WIMP search data, a slightly wider nuclear recoil band is masked off until after all cuts are defined and expected efficiencies computed to create a blind analysis technique.

In figure 2 there is also a class of electron recoil events which occur within a few microns of a detector surface (black crosses). In the absence of a calibration source, these could come from beta-emitters on the surface. Our radioactive sources provide such a population when betas are ejected from a nearby surface by incident gammas. For surface events, the charge collection is incomplete and thus the yield is reduced. However, these events also have a larger fraction of ballistic phonons (due to faster down-conversion near a surface) making for a faster risetime. Thus, timing cuts can be used to further isolate this population from the nuclear recoils. A timing parameter formed from phonon risetime and delay time (relative to the ionization signal) is plotted on the x-axis, with a dotted line demonstrating a simple background rejection cut. The location of the timing cut is determined using the calibration data prior to looking at the search region in order to end up with a background of ~ 1 leakage event within the box. Thus, we are not (yet) limited by surface beta background; we can always make the cut stricter as our mass and exposure time increases. We have also developed analyses based on χ^2 fits and neural network training to a multi-dimensional array of timing and energy partition parameters which can distinguish background and signal populations.

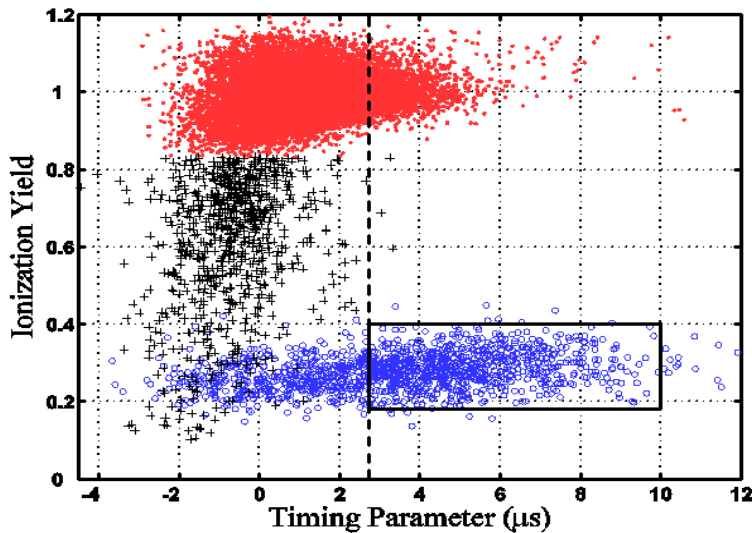


Figure 2. Ionization yield versus timing parameter for the middle Ge detector of Tower 2. Electron recoils in the bulk (red dots) produced by gammas from a ^{133}Ba source and nuclear recoils (blue circles) produced by neutrons from a ^{252}Cf source are well-separated in yield, but surface electron recoils (black crosses) require an additional timing cut (dotted line) to separate the populations.

3. Soudan Installation and Data-taking

The detector towers are placed inside the icebox which has room for seven towers of six detectors each, arranged in a hexagonal pattern. Figure 3 shows an assembled tower being inserted into the innermost can, connected to the mixing chamber of the refrigerator by a solid copper finger. A set of five nested low-radioactivity copper cans are individually thermally-coupled to the various temperature stages of the dilution refrigerator. The detector volume is cooled efficiently by conduction through the copper stems but kept away from all cryogenic liquids and any radioactivity in the commercial refrigerator itself.

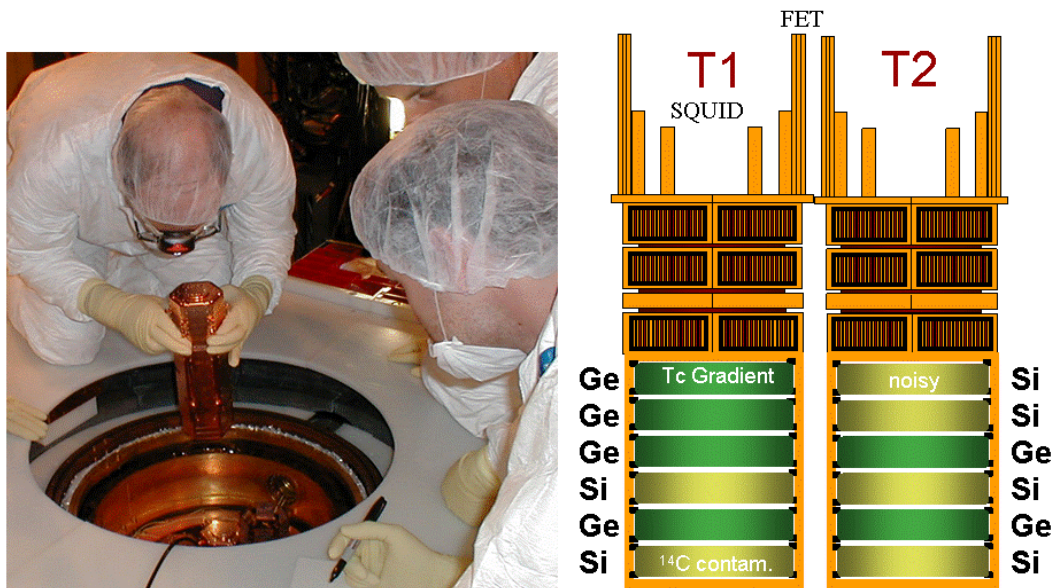


Figure 3. Left: One tower of 6 detectors being installed in the CDMS cryostat. Right: The arrangement of detectors used for the 2004 2-tower run.

Both Ge and Si detectors are stacked in two towers in the configuration shown in figure 3. Individual detectors are arranged in the bottom portion of the tower with 2 mm separation and no intervening material. Then the cold electronics for the ionization channels (FETs) and phonon channels (SQUIDs) are mounted on the top of the tower, which has surfaces at 4 K and 600 mK. Striplines connecting individual detector stacks to the room-temperature front-end electronics run out through an electronics stem.

Surrounding the icebox is a cylindrical inner polyethylene shield 10 cm thick, followed by 25 cm of lead and another 50 cm of polyethylene. This passive shielding is effective at removing neutrons and other radioactivity produced by the cavern walls, as well as gammas produced in the lead shield itself. The whole structure is overlaid with a muon veto made of 40 overlapping 2" thick plastic scintillator panels, calibrated using light from a bank of blue LEDs. The active shielding is 99.98% efficient for through-going muons. The apparatus is located underground where the Soudan overburden of 2090 mwe reduces the muon flux to 1 per minute in our active veto shield.

The air volume between the outermost icebox copper can and inner poly shield is continually purged with compressed air that has been stored for at least 2 weeks to allow most of the activity from ^{222}Rn and its associated daughters to decay away. A helium dilution refrigerator provides cooling. Both are housed in an EMI/RMI-shielded clean room. A sophisticated cryogen control system was developed for remote use so that liquid helium and nitrogen transfers can be fully monitored and controlled from the surface.

Shielding is the primary means of removing neutron background, since neutrons create nuclear recoils, just like WIMPs, and thus cannot be eliminated by yield or timing cuts. At this depth, cosmogenic neutrons are expected to be 1-2 per year per kg, but are reduced by two orders of magnitude by the active muon veto shield, mostly by accompanying muons and shower fragments. We have a few other handles on neutrons. Multiply-scattered nuclear recoil events can be identified as neutrons. Since Ge and Si have similar scattering rates per nucleon for neutrons, but not for WIMPs (the WIMP-nucleon scattering rate is expected to be 5-7 times greater in Ge), running with both types of detector provides a means to evaluate any unshielded neutron background. In addition, the kinematics of neutron elastic scattering give a recoil energy spectrum scaled in energy by a factor of ~ 2 in Si compared to Ge, compared to <1 for WIMP elastic scattering.

4. Experimental Limits

A run with one operating tower took place from October 11, 2003 to January 11, 2004 [5]. This run comprised 52.6 good live days. A second run from March 25-August 8, 2004 [6] consisted of 74.5 live days with the two tower configuration shown in figure 3. Energy calibrations to better than a few percent were performed using a ^{133}Ba gamma source with distinctive lines at 356 keV and 384 keV. Observation of the predicted energy spectrum from a ^{252}Cf source confirmed the energy scale for the nuclear recoils. To guarantee stability of operation and effective neutralization of the crystals during the WIMP search runs, the gamma band and the region above the nuclear recoil band of the WIMP search data were continuously monitored.

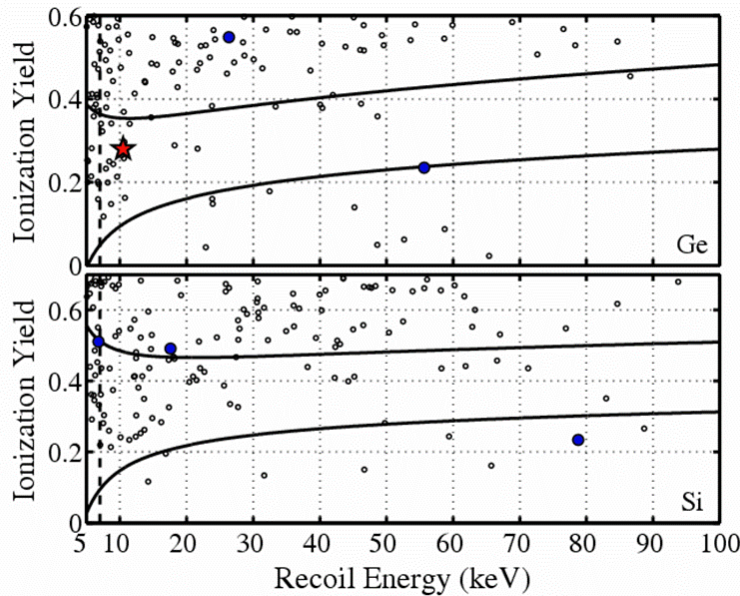


Figure 4. Ionization yield versus recoil energy for 1.25 kg of Ge and 0.4 kg of Si in the 2-tower run, prior to applying the timing cut. The signal region consists of recoil energies exceeding 7 keV, shown with a vertical dashed line, and yields between the curved lines (defined prior to unmasking using calibration data). Bulk-electron recoils with yield near unity are above the vertical scale limits.

In figure 4, the final revealed WIMP search data before applying the timing cut is plotted with respect to recoil energy. All 5 good Ge detectors are summed together in the top plot and all 4 good Si detectors in the bottom. One Si detector with ^{14}C contamination and a Si and Ge detector with poor phonon performance were excluded prior to unmasking the signal region. Events which passed the timing cuts are shown as blue circles, but only one (star) is within the nuclear-recoil band. This is consistent with our expected total of 0.4 ± 0.3 Ge (1.2 ± 0.6 Si) surface electron recoil events which could be misidentified as nuclear recoil events, an estimate based on leakage fractions in a sample of multiple detector events (not necessary to blind, as WIMPs will not multiply scatter). Monte Carlo simulations predict that background due to cosmogenic neutrons that escape detection by the active veto is negligible at this exposure.

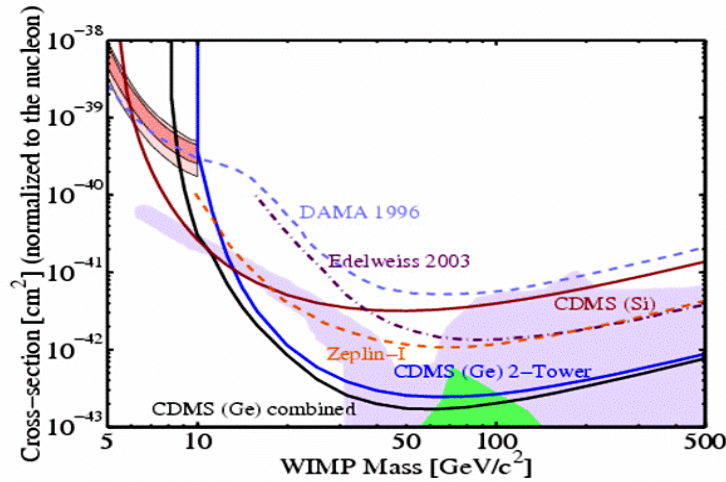


Figure 5: WIMP-nucleon cross section upper limits (90% C.L.) versus WIMP mass for the combined runs in Si and Ge down to 7 keV recoil energy and for the tower 2 Ge run on its own down to 10 keV. Supersymmetric models allow the largest shaded (light-blue) region [7], and the smaller shaded (green) region [8]. The shaded region in the upper left (see text) is from DAMA [9], and experimental limits are from DAMA [10], EDELWEISS [11], and ZEPLIN [12].

Cross sections calculated from the Ge and Si analyses using standard assumptions for the galactic halo [13] are found in figure 5. The strictest limit comes from combining the two Ge CDMS runs, including low energy recoil bins from 7-10 keV, to give a WIMP-nucleon cross section of $< 1.6 \times 10^{-43} \text{ cm}^2$ at the 90% C.L. for a WIMP mass of $60 \text{ GeV}/c^2$, a factor of 2.5 below our previously published limits. This new Ge limit constrains some minimal supersymmetric (MSSM) parameter space [7] and for the first time excludes some parameter space relevant to constrained models (CMSSM) [8]. The 2-tower Ge run alone provides the curve above that, where we restrict ourselves to data bins decided upon before unblinding. The 7-100 keV Si data from the 2-tower CDMS run limits the WIMP-nucleon cross-section to $< 3 \times 10^{-42} \text{ cm}^2$ at the 90% C.L. at a WIMP mass of $60 \text{ GeV}/c^2$, excluding new parameter space for low-mass WIMPs, including a region compatible with interpretation of the DAMA signal (2-6 and 6-14 keVee bins) as scattering on Na [9].

CDMS also has sensitivity to spin-dependent WIMP-nucleon interactions via the presence of non-zero spin isotopes in our natural Ge and Si crystals, namely 7.73% ^{73}Ge (spin=9/2) and 4.68% ^{29}Si (spin=1/2). Each isotope contains a single unpaired neutron, making CDMS much more sensitive to spin-dependent interactions with neutrons than with protons. Combining CDMS data down to 7 keV from both runs yields a total of 11.5 (1.7) raw kg-days ^{73}Ge (^{29}Si) exposure with a single background event seen in the Ge data. In combination with CRESST I [14], the pure WIMP-neutron limit (see figure 6) is inconsistent with an interpretation of the DAMA/NaI annual modulation amplitude in terms of such interactions within the standard halo model (see also [15]). CDMS does not currently set the strongest limits in the pure WIMP-proton case, but has begun to explore the regions of this parameter space. More importantly, the use of two active isotopes can narrow the $a_p - a_n$ plane for general models without pure couplings and yield constraints on the relationship between the two, especially when combined with constraints from other experiments.

We are currently cooling down for a run expected to start in January 2006 with 3 additional towers comprising 5 more Si detectors and 13 more Ge detectors. This run will last for 1-2 years and extend our reach by an order of magnitude in sensitivity.

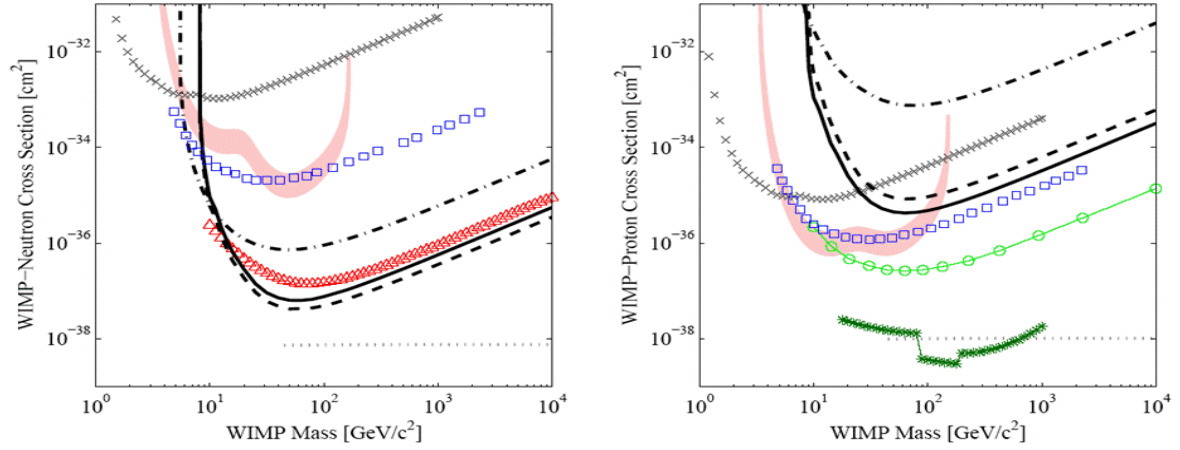


Figure 6. Upper limit contours (90% confidence level) for the cases of pure neutron (left) and pure proton (right) coupling. CDMS limits (black) come from the 2 Soudan runs combined for Ge (solid) and Si (dash-dot). Dashed curves represent Ge limits using the alternate form factor from [16]. As benchmarks, we also include interpretations of the DAMA/NaI annual modulation signal [17] (filled regions are 3σ -allowed) and limits from other leading experiments: CRESST I [14] (x's), PICASSO [18] (squares), NAIAD [19] (circles), ZEPLIN I [20] (triangles), and Super-Kamiokande [21] (asterisks; an indirect search, based on different assumptions).

References

- [1] Spergel D N et al. (WMAP Collab.) 2003, *Astrophys. J. Suppl.* **148** 175 and Tegmark M et al. (SDSS Collab.) 2004 *Phys. Rev.* **D 69** 103501
- [2] Steigman G and Turner M S 1985 *Nucl. Phys.* **B 253** 375
- [3] Jungman G, Kamionkowski M, and Griest K 1996 *Phys. Rep.* **267** 195 and Bertone G, Hooper D, and Silk J 2005 *Phys. Rep.* **405** 279
- [4] Akerib D S et al. (CDMS Collab.) 2005 *Phys. Rev.* **D72** 052009
- [5] Akerib D S et al. (CDMS Collab.) 2004 *Phys. Rev. Lett.* **93** 211301
- [6] Akerib D S et al. (CDMS Collab.) 2005 *accepted by Phys. Rev. Lett.* (Preprint arXiv:astro-ph/0509259 and arXiv:astro-ph/0509269)
- [7] Bottino A, Donato F, Fornengo N and Scopel S 2004 *Phys. Rev.* **D69** 037302
- [8] Ellis J, Olive K, Santoso Y and Spanos V C 2005 *Phys. Rev.* **D71** 095007
- [9] Gondolo P and Gelmini G 2005 *Phys. Rev.* **D71** 123520
- [10] Bernabei R et al. (DAMA Collab.) 1996 *Phys. Lett.* **B389** 757
- [11] Sanglard V et al. (EDELWEISS Collab.) 2005 *Phys. Rev.* **D71** 122002
- [12] Akerib D S et al. (UK Dark Matter Collab.) 2005 *Astropart. Phys.* **23** 444
- [13] Lewin J D and Smith P F 1996 *Astropart. Phys.* **6** 87
- [14] Angloher G et al. (UKDMC) 2002 *Astropart. Phys.* **18** 43
- [15] Savage C, Gondolo P and Freese K 2004 *Phys. Rev.* **D70** 123513
- [16] Ressel M T et al. 1993 *Phys. Rev.* **D48** 5519
- [17] Bernabei R et al. 2003 *Riv. Nuovo Cim.* **26N1** 1
- [18] Barnabe-Heider M et al. (PICASSO) 2005 *Phys. Lett.* **B624** 186
- [19] Akerib D S et al. (UKDMC) 2005 *Phys. Lett.* **B616** 17 (Preprint arXiv:hep-ex/0504031)
- [20] Kudryavtsev V A (UKDMC) 2004 *5th Int'l Workshop on the Identification of Dark Matter, Sept 6-10 Edinburgh, Scotland*
- [21] Desai S et al. (Super-Kamiokande) 2004 *Phys. Rev.* **D70** 08352